INSTITUTO DEL MAR DEL PERU

Boletín

ISSN - Q 378 - 7699
VOLUMEN EXTRAORDINARIO

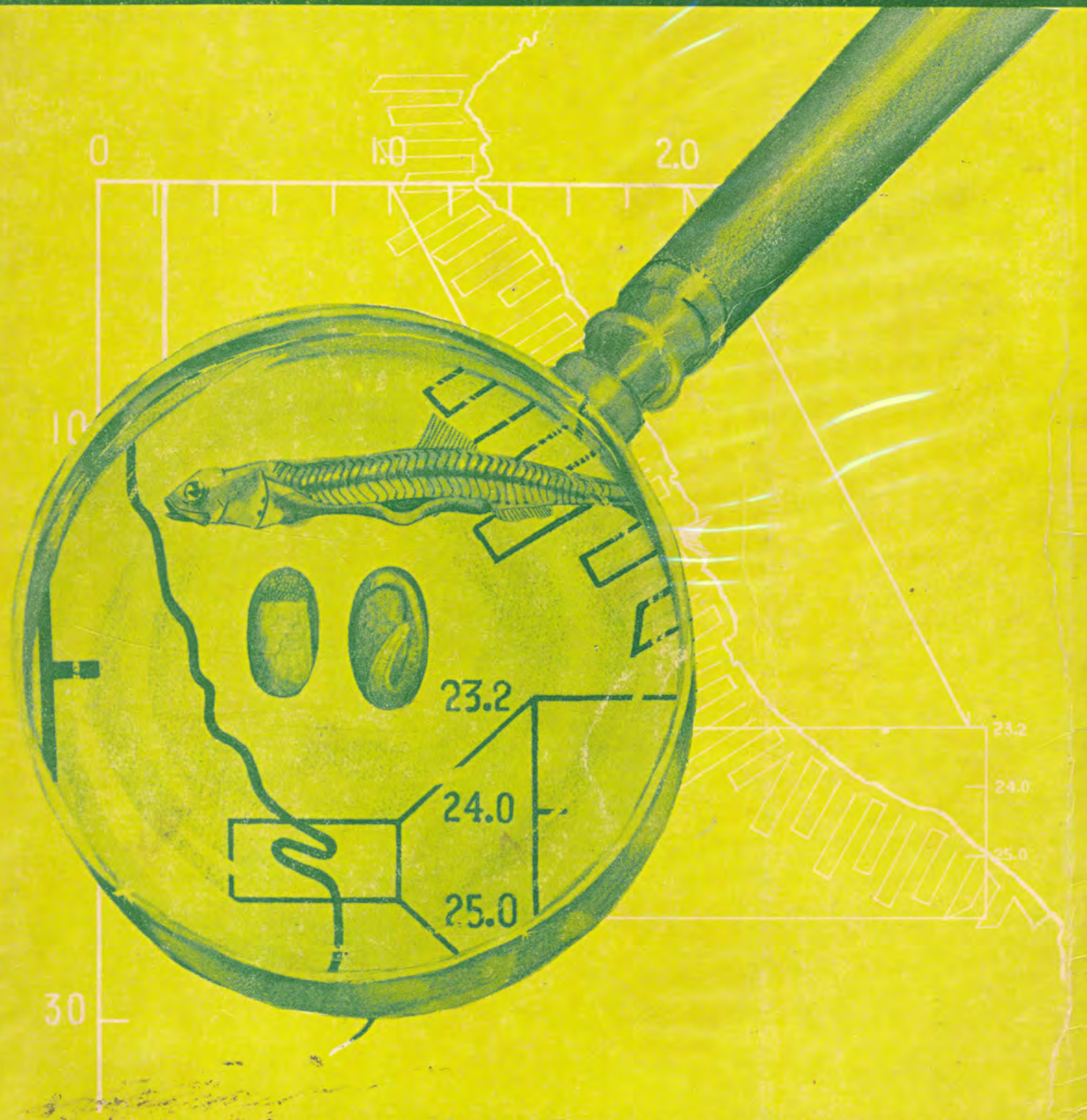

INVESTIGACION COOPERATIVA DE LA ANCHOVETA Y SU ECOSISTEMA - ICANE - ENTRE PERU Y CANADA CALLAO 1981 PERU

SPATIAL AND TEMPORAL VARIABILITY OF CHLOROPHYLL DISTRIBUTIONS AND GEOSTROPHIC ESTIMATES ON THE PERU SHELF AT 9° S

Alex W. Herman
Department of Fisheries and Oceans, Atlantic Oceanographic Laboratory Bedford Institute of Oceanography, Dartmouth, Nova Scotia B2Y 4A2

ABSTRACT

Profiles of chlorophyll a, temperatures and salinity were measured over the Peru shelf at 9°S. Data were collected with a Batfish vehicle profiling in a sawtooth pattern over a cycle distance of~1 km at a depth ranging from near surface to~80 m. Following a discussion of the validity of geostrophy in the cross shelf direction geostrophic estimates of the alongshore velocity field on the shelf were made and from observations of the spatial and temporal variability of σ_t it was determined that geostrophic estimates when obtained by conventional sampling, that is, using CTD profiles with spacings of~10 km may be grossly misleading. The variability in measured chlorophyll distributions was also high and appeared to be related to the variability in the geostrophic field estimates. Chlorophyll maxima also appeared to be highly correlated with salinity maxima even though vertical salinity changes were extremely small (~0.1°/oo); the correlation may have represented an association between high chlorphyll and Subtropical Surface Water particularly in the region from the mid-shelf to the outer shelf. The static and dynamic vertical stability were also estimated for possible vertical mixing mechanisms operating in the euphotic zone.

RESUMEN

La clorofila a, temperatura y la salinidad se midieron en varios perfiles sobre la plataforma del Perú a los 9°S. Los datos se colectaron mediante el Batfish en zig-zags de ± 1 km de amplitud y a profundidades de aproximadamente 80 m desde cerca de la superficie. Luego de discutir la validez de los métodos geostróficos se hicieron estimaciones del campo de velocidad a lo largo de la costa en la plataforma y a partir de observaciones de la variabilidad espacial y temporal de σ_t se determinó que los estimados geostróficos obtenidos mediante muestreos convencionales, esto es, usando perfiles de CTD espaciados por más o menos 10 km pueden conducir a gruesos errores. La variabilidad en la medición de las distribuciones de clorofila fue también alta y aparentemente relacionada con la variabilidad de los estimados del campo geostrófico. Los máximos de clorofila también aparecieron estar altamente correlacionados con los máximos de salinidad aunque los cambios verticales de salinidad fueron muy pequeños (aproximadamente 0.1°/oo); la correlación puede haber representado una asociación entre altos niveles de clorofila y las Aguas Superficiales Subtropicales especialmente en la región de la mitad de la plataforma hacia afuera. La estabilidad vertical estática y dinámica fueron tan bien estimadas por la posibilidad de que mecanismos de mezcla vertical operen en la zona eufótica.

INTRODUCTION

Circulation near the coast of Peru is characterized by predominantly poleward flow on the shelf and equatorward flow confined to a shallow wind-drift surface layer (Wooster and Gilmartin 1961). Upwelling on the shelf (north of 15°S) results in the Peru undercurrent flowing south with the Peru countercurrent and intruding over the continental shelf. In this region, upwelling is restricted to depths of~100 m (Wyrtki 1963). The region of 15°S has been widely studied (Eber et al., 1968) and has received more attention than areas to the north where upwelling is less persistent (Guillen, 1979). Richman and Smith (1980) have proposed the enhancement of oxygen depletion between 6° and 11° S based on a two-layer model of shallow Ekman-driven upwelling.

The coastal waters of Peru between 6° and 11° S were the subject of the biological project, ICANE (Investigacion Cooperativa de la Anchoveta y su Ecosistoma) during November 1977 which was designed to study anchovy larvae and their ecosystem. This paper describes the variability of the geostrophic circulation and chlorophyll distribution, the interaction of the latter two and possible

vertical mixing mechanisms estimated from static and dynamic stability. Following a description of the instrumentation and sampling methods, profiles of temperature and salinity contoured on depth (to ~100 m) are presented for several transects taken inshore and across the entire shelf as well as a transect taken northwards. The corresponding chlorophyll profiles are also presented. From the corresponding density profiles the estimated geostrophic velocity field across the shelf is presented along with the method of analysis. The temporal variability in the density field of a 20 km section of this field was demonstrated by continuos towing over a 15 hr period and provides insight into the problems of geostrophic estimates in this shelf region using conventional sampling techniques. Estimates of Brunt-Väisälä frequencies and Richardson numbers are made nearshore and offshore and provide a basis for possible vertical mixing mechanisms in the euphotic zone.

Instruments and Methods. Rapid and high resolution profiling was accomplished with a 'Batfish' vehicle (Dessureault 1976) towed in a sawtooth pattern. The vehicle carries a digital CTD (Model 8705, Guildline Instruments, Smiths Falls, Canada) to measure salinity, temperature and depth, a Variosens fluorometer (Impulsphysik GmbH, Hamburg, West Germany) to measure chlorophyll **a**, and an electronic **in situ** zooplankton counter (prototype). The accuracy and noise specifications are measured in a standards laboratory at the Bedford Institute of Oceanography prior to and following each cruise. The fluorometer has a measuring range of ~0.3 mg m^{-3} (±15%) to ~30 mg m^{-3} (±3%) and the zooplankton counter sizes animals in the diameter range of ~0.4 to 4 mm. The operating characteristics of the instruments and their deployment on Batfish have been described elsewhere (Herman and Denman 1976; Herman and Dauphinee, 1979). During normal operations, the Batfish is towed at speeds of ~3 m s^{-1} and cycled at depths of ~2 to 100 m with diving rates of ~0.4 m s^{-1}.

The Variosens fluorometer was used in conjunction with a Turner 111 fluorometer (flow-through system), the latter providing a reference calibration (Herman 1977) for the Variosens. Prior to and following the cruise, the Variosens was calibrated in the laboratory simultaneously with a Turner 111 fluorometer using laboratory grown cultures. At sea, vertical profiles of chlorophyll were made by pumping sea water to the Turner fluorometer from the surface to a depth of 35 m at 5 m intervals. Replicate one litre seawater samples were then filtered from the effluent of the Turner fluorometer and chlorophyll was determined by the extraction method described by Yentsch and Menzel (1963). From the linear relationship between fluorescence and chlorophyll, the sea calibration (as distinct from the lab calibration) for the Turner fluorometer was subsequently made. After comparing the slopes of the fitted calibration lines for both the laboratory and sea calibration, the change in fluorescence intensity per unit mass of chlorophyll (from lab to sea) was determined. The procedure provided not only the sea calibration for the Variosens but also monitored the changes in sea calibration over the cruise period.

Shelf Profiles. The operational area and transects sampled with the Batfish are shown in Fig. 1. The onshore-offshore transects were chosen approximately normal to the coastline and bounded by positions 78°48'W, 9°19'S and 79°26'W, 9°42'S (approximately 45 n.m. in length) and the alongshore transect was chosen parallel to the coast-

Fig. 1 Location of work area at 9°S on the Peru shelf. Batfish transects are indicated normal and parallel to coastline. The cross shelf transects were sampled during the period of Nov. 15-23, 1977 and the alongshore transect was sampled on Nov, 16, 1977.

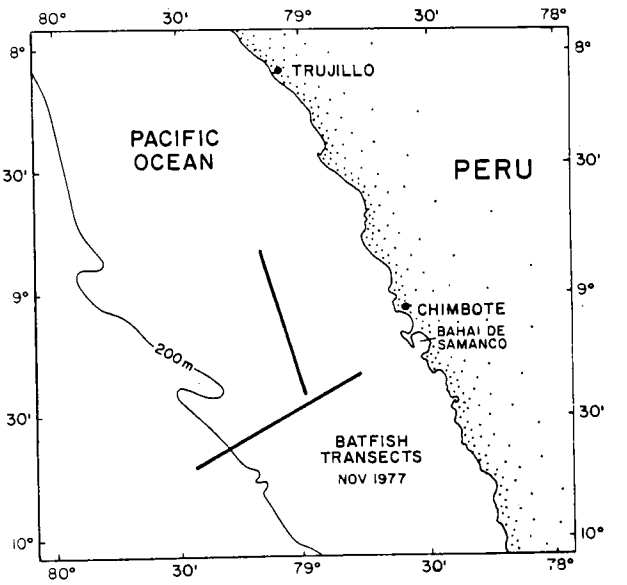

line bounded by positions 78°57'W, 9°23'S and 79°10'W, 8°50'S (approximately 35 n.m. in length). The across-shelf transect extended from ~25 km offshore to the shelf break at ~ 300 m depth. Sampling took place during three periods: on November 15-16 a tow over the inshore half of the across-shelf transect and an alongshore tow to the north were made; on November 18 an inshore tow east of 79° was made; and on November 22-23 a tow extending the full length of the across-shelf transect was made. For the most part, tows were not continuous due to interruptions caused by fishing boat traffic (particularly offshore) and to the maintenance requirements of the Batfish plankton nets. These interruptions caused data gaps of ~2 n.m. in length.

Temperature data contoured on depth for the three periods are shown in Fig. 2 (a-c) for the across-shelf transect plotted with the corresponding salinities in Fig. 3 (a-c). Data gaps are indicated by the dashed line contours. The most extensive coverage across the shelf was in the temperature and

Fig. 2 (a) Temperature contoured on depth for the across shelf transect on Nov. 15-16. Batfish depth traces are partially indicated on top and bottom.

(b) Temperature contoured for the transect of Nov. 18.

(c) Temperature profile from the outer edge of the shelf sampled on Nov. 22.

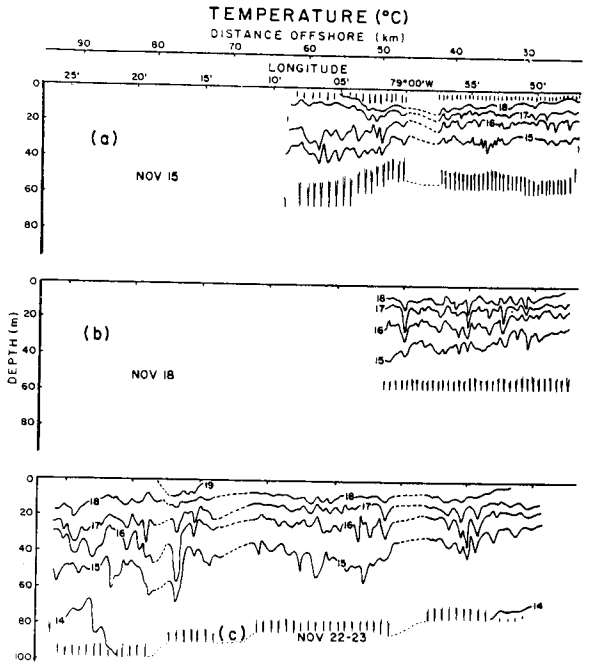

Fig. 3 (a,b,c,) Salinity profiles for the across shelf transect sampled for three periods: (1) Nov. 15-16, (2) Nov. 18, and (3) Nov. 22-23.

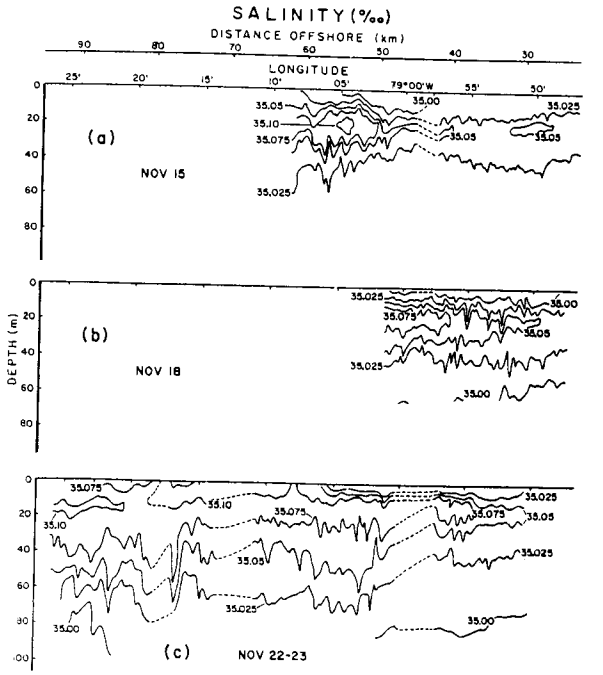

salinity profiles of Fig. 2 (c) and 3(c) respectively. The isolines in both figures sloped upwards on average towards the onshore direction and is conventionally indicative (Richman and Smith, 1980; Guillen **at al.**, 1977) of shallow upwelling from~50 m as seen, for example, from the offshore depth of the 15°C isoline. The salinity contrasts over depth (0-100 m) were quite small (~0.1°/oo) and therefore temperature can be taken representative of the density (σ_T) field. There was a distinct subsurface salinity maximum inshore in all three transects. This signified that the surface mixed layer was shallow (< 10 m) and if indicative of the Ekman transport layer, it would be characteristically cooler and fresher than intermediate depths. In contrast to the salinity, a lower temperature signal which would be expected if upwelling were occurring was not observed for the surface mixed layer and this may be a consequence of surface heating ($\overline{Q} \sim 160$ J m^{-2} s^{-1} for November 1977; Glen Harrison, personal comunication). However, the offshore to onshore surface temperature gradient was more indicative of upwelling as temperature decreased (19°C to 18°C) moving inshore [Fig. 2 (c)] and this was also observed for the surface salinity gradient which also decreased (35.1-35.025°/oo) inshore. A tongue with a salinity $>$ 35.075°/oo was seen to protrude inshore at a depth of~20 m at the base of the surface mixed layer [Fig. 3 (c)]. The tongue appeared to progress inshore over the seven-day period as indicated by the sequence of Fig. 3 (a-c).

The corresponding chlorophyll sections are shown in Fig. 4 (a-c). The first two transects [Figs. 4 (a,b)] indicated the chlorophyll maximum de-

Fig. 4 (a,b,c) Chlorophyll profiles for the cross shelf transect taken simultaneously with the T,S profiles of Fig. 2 and 3.

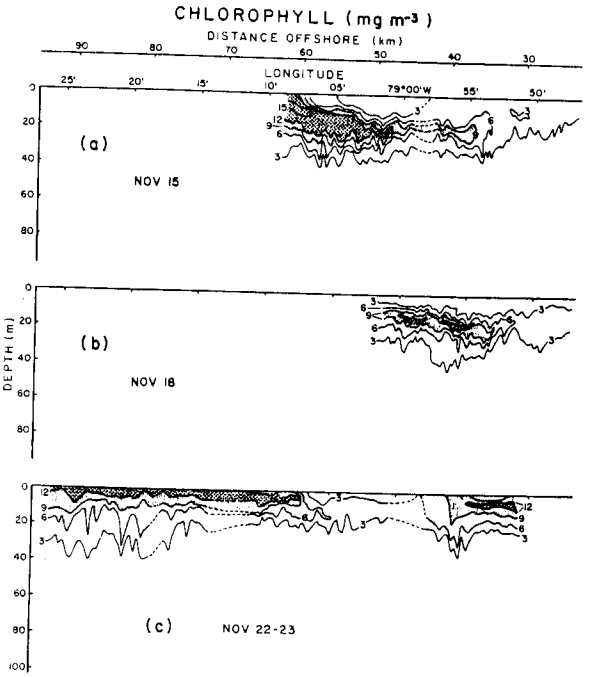

creased (~12 mg m^{-3} to ~3 mg m^{-3}) inshore. Farther inshore, pumping stations at 79°40'W showed chlorophyll maximum concentrations of ~3 mg m^{-3}. The chlorophyll contours in the first two transects are strongly correlated with salinity contours. For example, in Fig. 4 (a), the surface lens of low chlorophyll bounded by the contour of 3 mg m^{-3} was correlated with a low salinity lens bounded by 35.00°/oo as seen in Fig. 3 (a). Also in the first two transects the inshore subsurface chlorophyll maximum corresponds to the high salinity tongue (≥35.05°/oo) protruding inshore at ~20 m depth. A plot of chlorophyll–salinity is shown in Fig. 5 for a Batfish profile taken at 79°03'W of Fig. 4(a). The chlorophyll and salinity maximum corresponded, and within the surface mixed layer chlorophyll bore a near-linear relationship with salinity.

Fig. 5 Chlorophyll vs salinity for a single Batfish profile from 3-80 m depth. The chlorophyll maximum was seen to correspond to a salinity maximum.

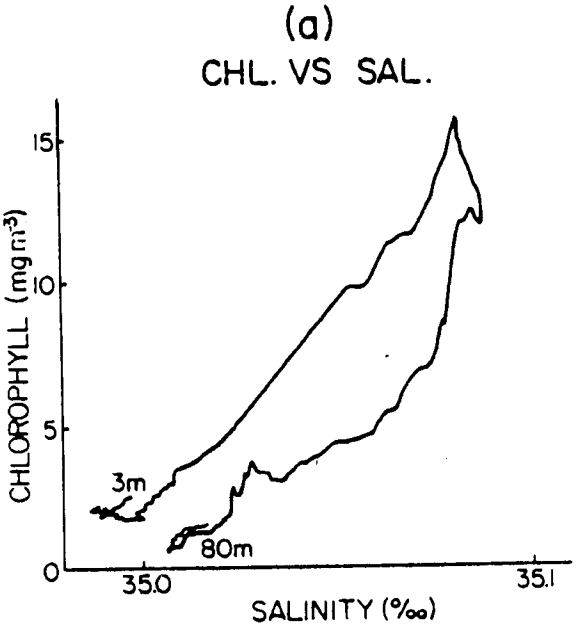

Further samples of the chlorophyll-salinity relationship are presented in Figs. 6(a-c) for all three transects. Single Batfish profiles were selected from approximately equidistant positions and are represented from left to right as moving onshore. The relationship of the chlorophyll-salinity maximum generally held except perhaps for inshore regions.

The salinity maximum can be related to the local water masses. In this region over the shelf there are primarily two water mass types: (1) Subtropical Surface Water characterized (Wyrtki, 1963) by salinities ≤35.1°/oo (or ≥35.05°/oo, Barber **et al.**, 1971) and temperatures between 17° and 20°C and originating in the subtropical region of the South Pacific Ocean and brought by circulation into the region off Peru; (2) Equatorial Subsurface Water characterized (Wyrtki, 1963) by salinities ≤35.1°/oo and temperatures between 7° and 17°C; it is essentially part of the Peru Undercurrent supplying coastal upwelling. The salinity transition between the two water masses was clearly not distinct in our measurements but occured within the region of ~35.0 and 35.1°/oo The high salinity tongue may be subtropical Surface Water (or a mixture thereof) characterized by low nutrients (Guillén and de Rondan, 1973) which is in agreement with nutrient data for this cruise indicating low surface nutrients (nitrates ~5 mg-at m^{-3}) to ~20 m depth at the shelf break (Pocklington **et al.**, 1978). Subtropical surface water is also characterized by low chlorophyll **a**, low production (Guillén **et al.**, 1973; Guillén and Rondan, 1973; Strickland **et al.**, 1969; and Barber **et al.**, 1971) and a high abundance of coccolithophores. For our sampling period, the Batfish data indicated high chlorophyll **a** which was inconsistent with previous data. Also other experiments (Harrison **et al.**) indicated low production offshore where P_B^{MAX} ~2 mg C (mg Chl **a**)$^{-1}$ hr^{-1}. There was also evidence (N. Ochoa, G. Harrison private communication) that the abundance of coccolithophores increased by an order of magnitude offshore (west of 70°W) whereas the diversity and abundance of diatoms decreased by nearly the same order. The salinity – chlorophyll maximum associated with subtropical surface water would therefore appear to be anomalous and unexplained.

In Fig. 4 (c), high chlorophyll concentrations (~12 mg m^{-3}) were measured in the surface layers (<10 m) offshore where phaeopigments comprised ~20°/o of the total pigment composition and in deeper waters (~30 m) where chlorophyll levels were still significant (~4 mg m^{-3}), the phaeopigments comprised ~60°/o. It is difficult to ascertain from the data whether or not the surface maximum contained detrital chlorophyll or old phytoplankton populations; however, there was evidence from the electronic zooplankton counter measurements that grazing occurred just above (~5 m) the chlorophyll maximum which was located at ~15 m depth. Grazing could then account for the high phaeophytin concentrations located below the zooplankton layer at ~10 m depth. Chlorophyll levels were still significant at depth, e.g. (~2 mg m^{-3} at 40 m depth) and although growth would be light limited, there is evidence (Guillén and de Rondan, 1973) that 'shade adapted' phytoplankton populations may account for these concentrations even in low light intensities. Nutrients were high at these depths (nitrates ~20-30 mg-at m^{-3}) which corresponded to the base of the thermocline and coincided with the depth region where it was estimated that strong vertical mixing due to shear instabilities may occur. This point is discussed later in the section on 'Vertical Stability'.

Following the second transect on Nov. 18, chlorophyll concentrations east of ~79°00'W (at 9°00'S) dramatically decreased to ~1 mg m^{-3}

as determined from pumping stations. These inshore levels began to recover again on November 20 and a Batfish transect was subsequently made on November 22-23 in the inshore starting from the edge of the shelf. The temperature, salinity, and chlorophyll profiles are shown in Figs. 2 (c), 3(c), 4(c). Here the inshore chlorophyll structure east of 79°05'W changed dramatically although at 79°05'W the surface outcropping of salinity contours bounding the wind-mixed layer still corresponded to the outcropping of the chlorophyll contours. It was believed that in the inshore region east of 79°00'W the observed chlorophyll variability was caused by poleward advection as indicated by the N-S chlorophyll gradient of Fig. 7(c).

The contoured profiles of temperature, salinity, and chlorophyll for the alongshore transect northward (see Fig. 1) are shown in Fig. 7 (a, b, c). There are two features present in the profiles that require elaboration. Firstly, there was a ~5 to 10 km section of extremely low chlorophyll (<1 mg m^{-3}) at 9° 15'S and secondly, there was a high salinity tongue of 35.075°/oo situated between 9°00'S and 9°12'S at ~20 m depth. The salinity profile (as well as temperature) is assumed to have approximately the same cross shelf structure as that measured in Fig. 3 (a, b, c). Therefore, if salinity at ~20 m depth increased northward as seen in Fig. 7(b) then the observation that the salinity tongue of 35.075°/oo was moving inshore in Fig. 3 (a,b, c) over time was consistent with expected poleward advection. Also, poleward advection of the northern region of low

Fig. 6 (a-c) Chlorophyll vs salinity profiles plotted moving onshore for several positions within the three shelf transects correspondin to Fig. 2-4. Generally the chlorophyll maximum was seen to correspond to the salinity maximum.
(d) Same as (a-c) except plotted for a northerly transect corresponding to Fig. 7.

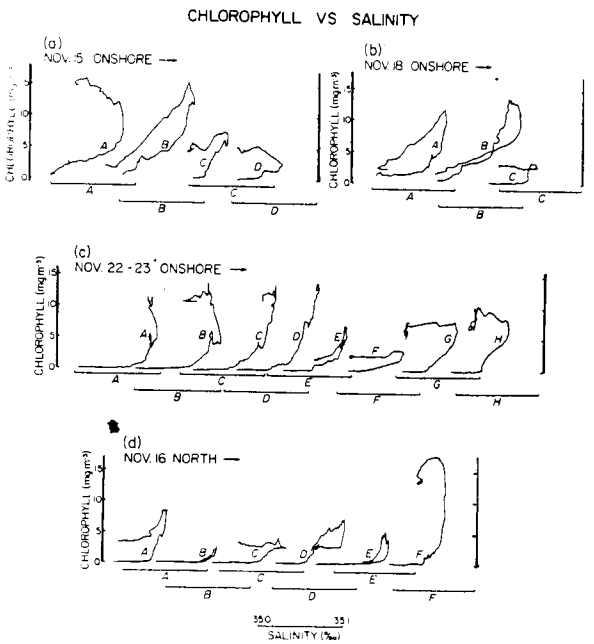

chlorophyll ≤ 1 mg m^{-3} in Fig. 7 (c) was consistent with the low chlorophyll ≤ 1 mg m^{-3} measured on November 19-20 at the inshore region between 78°50' – 79°00'W at 9°00'S. The east-west extent of the structure for the low chlorophyll region in Fig. 5 (a) is not known. Based on horizontal distance and time measurements, the magnitude of flow (in the upper layers, say, ~ 30 m) required to move both the low chlorophyll region or salinity tongue into our sampling area for the given time period is estimated at –4 cm s^{-1} (poleward).

GEOSTROPHIC CALCULATIONS

Baroclinicity and Botton Friction. The validity of the thermal wind equation for the Peru shelf has been investigated extensively by Brink **et al.** (1978) at 15°S. If the alongshore flow is geostrophically balanced, then its fluctuations will produce predictable fluctuations in the density (or temperature) field. Brink measured the strength of coupling between the alongshore flow v and the cross shelf gradient of T by means of empirical orthogonal functions. Data consisting of v, T were obtained from current meter moorings situated; (1) inshore, ~3 km from the coast; (2) mid-shelf, ~12 km offshore; and (3) over the shelf slope, ~3 km from the coast; (2) mid-shelf, ~12 km offshore; and (3) over the shelf slope, ~28 km offshore as seen in Fig. 2 of Brink **et al.** (1978) and measured over three phases during the period of 25 March to 30 September 1976. He found that fluctuations in v were strongly baroclinic over the slope, intermediate at the inshore station, and non-baroclinic at mid-shelf during the first two phases. Mid-shelf baroclinicity was observed during the last phase and this was attributed by Brink to a decrease in botton friction measured by the local turbulent botton Ekman number (the ratio of Ekman layer depth to total fluid depth), which decreased from 1 to 0.5 in the last phase. The surface mixed layer for their experiment was measured from 30 to 50 m.

Another method to determine the validity of geostrophy is to examine the individual terms in the cross shelf momentum equation. If the balance is geostrophic, the inertial, non-linear and frictional terms must be much smaller than the Coriolis and pressure terms. In non-dimensional terms this means the time scales must be greater than the inertial period and the Rossby No. (the ratio of the non-linear terms to the Coriolis terms) must be smaller than 1. The botton Ekman number for our region was generated from Equation 4.2 of Brink **et al.** (1978) and was estimated at ~0.7, which implies that the effects of botton friction may be significant. However vertical stratification was stronger in our area; that is, vertical density gradients were 2 to 4 times larger than those estimated from the density sections of Brink **et al.** (1978) in Fig. 4.2 and were therefore suggestive of lesser effects of botton friction for our area.

We also consider the effects of non-linear

terms, that is, the ratio of non-linear and Coriolis terms otherwise called the Rossby number

$$R_O = U_f^{-1} L^{-1}$$

where U is an average alongshore flow (~10 to 15 cm s^{-1}) and L is the radius of deformation chosen at ~20 km. The Rossby number is ~0.3, which indicates that the effects of non-linear terms may also be significant in the momentum equation for governing the cross shelf flow.

These results together with those of Brink et al. (1978) suggest the main balance is geostrophic but significant contributions can be made by non-linear or botton friction terms. Recognizing these problems the geostrophic velocity field based on the Batfish profiles are calculated.

Data Analysis. The geostrophic velocity field was generated for the across-shelf transect using density profiles calculated from temperature and salinity profiles of Fig. 2(c) and 3(c). Due to the density of observations, a unique but simple method of preventing spatial aliasing, while retaining the best possible resolution, was used to integrate the thermal wind equation (Neuman and Pearson, 1966).

Figure 8(a) illustrates two Batfish tows in which up and down traces (indicated by arrows) have been selected as vertical profiles. Geostrophic calculations of velocity were made between pairs of density profiles separated by a distance X apart or equivalently denoted by N, the number of profiles between the pair (e.g. N = 20 as shown).

Fig. 7 (a) Temperature, (b) salinity, and (c) chlorophyll profiled for the northward transect shown in Fig. 1. The extremely high chlorophyll at the northern end was caused by a red tide event.

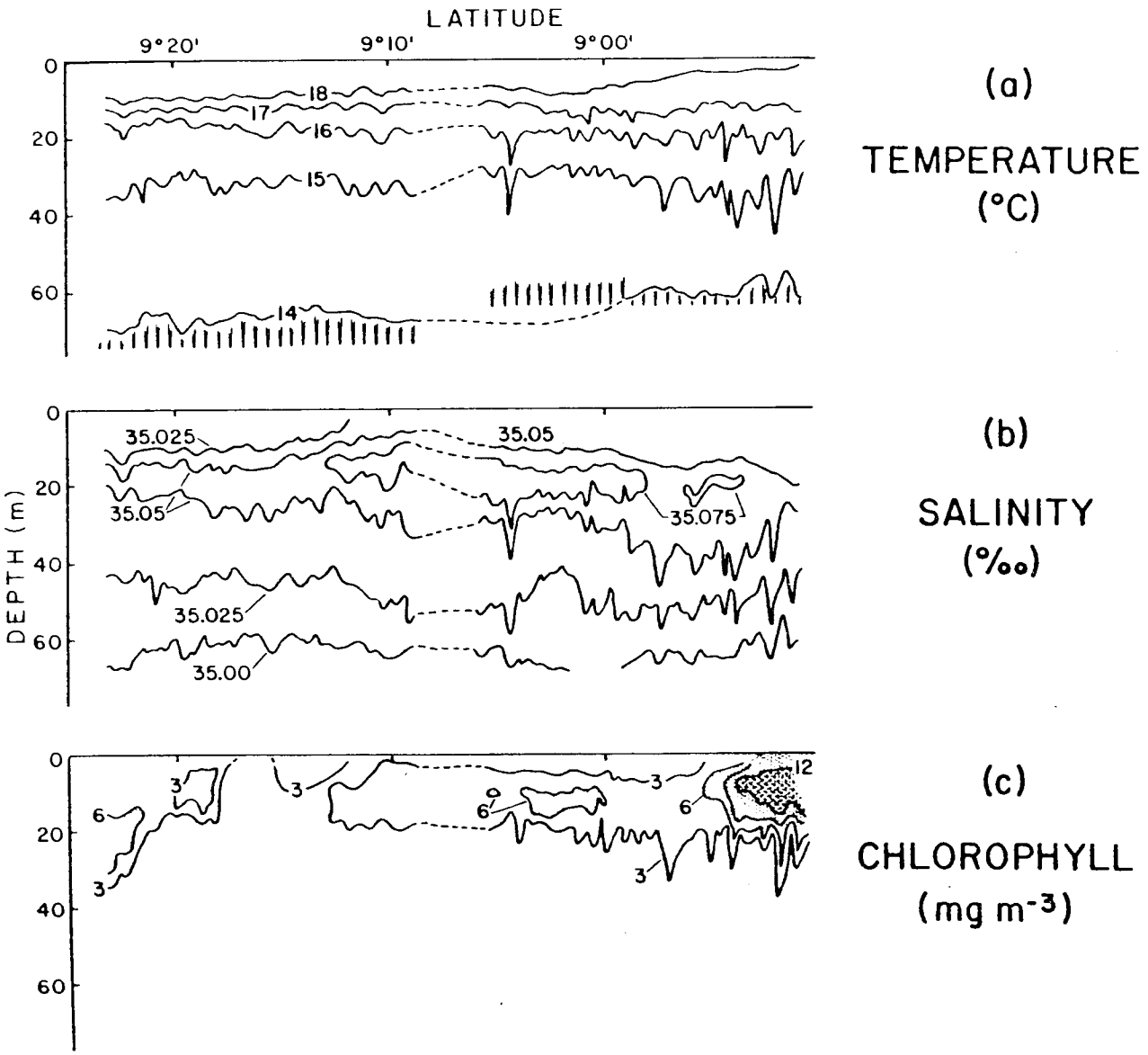

The number N was chosen to be even so that density pairs consisted of either pairs of up traces or pairs of down traces and due to their oblique (not strictly vertical) nature were therefore a constant distance apart. The first geostrophic calculation was accomplished by taking N_A = 2 and N_B = 22 as the second density pair and so on. The mean velocity profile was estimated therefore at a distance halfway between the density pairs, that is, at X/2 or equivalently at $N_B/2$. As the distance between each profile was ~0.5 km, the velocity profile was then estimated at the distance X/2 = 5 km for the latter example. Velocity profiles were also generated within the data gaps between two tows provided this distance (between the end of the last tow and the beginning of the next tow) was less than X, the distance requiered between density profile pairs. An example is given for the righthand side of Fig. 8(a).

The selection of the optimum value of N, the

Fig. 8 (a) Illustration of the method used in the geostrophic velocity calculations from Batfish density profiles. The mean velocity profile was calculated from pairs of density profiles separated by N profiles. Up and down Batfish traces are indicated by arrows.

(b) The mean standard deviation of the velocity field plotted against the distance between dentsity pairs used for the geostrophic calculations. The optimum distance between density pairs was chosen at 10 km where high wavenumber noise is minimized.

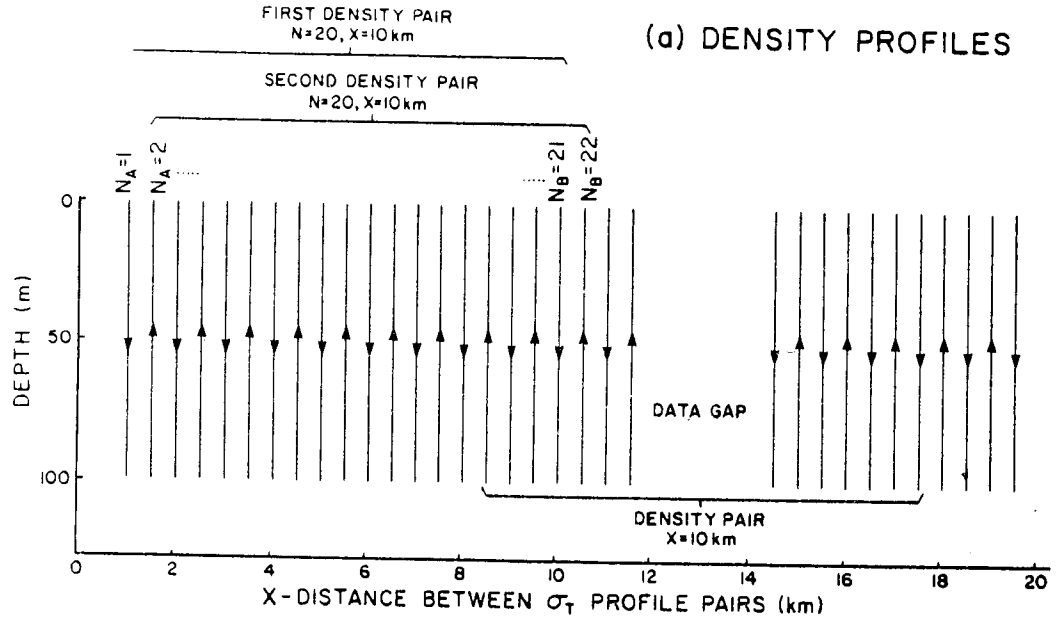

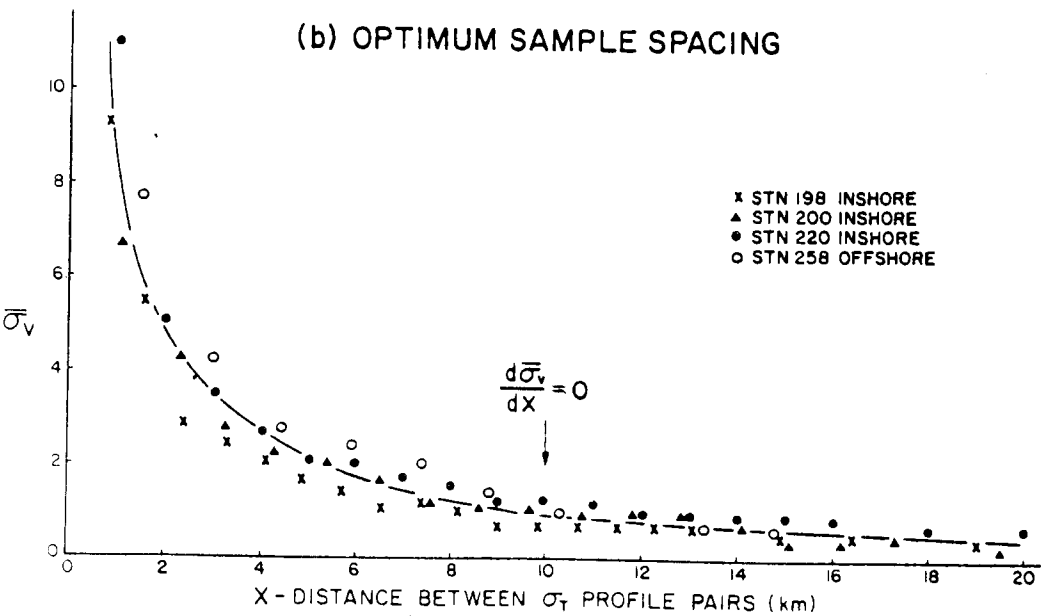

number of profiles between density profile pairs, required a statistical test. Small values of N (i.e. N = 2 or equivalently X = 1 km) meant the estimates of velocity would be contaminated by high wavenumber perturbations of the same approximate wavelength (1 to 2 km) and large values of N meant that more velocity data would be lost at either end of the tow (the loss corresponding to N/2 or X/2). First a single parameter was chosen that was sensitive to changes in the overall velocity field with X or N such that these changes diminished to zero as X or N was increased. A zero change signified a diminished influence of density variations caused by internal waves. For each vertical profile, a mean standard deviation was calculated from a mean vertical velocity field $\bar{V}$ using.

$$\sigma_i = \sum_j (V_j - \bar{V})^2 / n_d \qquad (1)$$

where V_j is the velocity at the j^{th} depth n_d is the number of depths used in the summation and σ_i is the mean standard deviation for the i^{th} profile. The mean field $\bar{V}$ was arbitrarily set to zero since we are concerned with change in the velocity field and not its absolute value. The mean standard deviation $\bar{\sigma}_V$ for the entire velocity field was then evaluated by averaging the standard deviations for the total number of profiles N_p in the velocity field and is represented by

$$\bar{\sigma}_V = \sum_{i=1}^{Np} \sigma_i / Np \qquad (2)$$

Therefore $\bar{\sigma}_V$ was evaluated for the entire velocity field as a function of X the distance between density profile pairs and the optimum X was chosen at $\partial\bar{\sigma}_V / \partial X = 0$. Figure 8(b) represents a plot of $\bar{\sigma}_V$ in Eq. 2 versus distance X for a variety of tows, three inshore and one offshore. The optimum distance X was chosen at 10 km where the change in $\bar{\sigma}_V$ was observed to rapidly approach zero. It was seen from Fig. 8(b) that there occurred a significant change of an order of magnitude in the estimates of velocity between X = 1 to 10 km. Roughly interpreted, the selection of 10 km spacing between stations reduced the high wavenumber signal (~1 km) contribution by an order of magnitude approximately 67% of the time (i.e. one standard deviation). Moreover, the selected spacing of 10 km between Batfish (vertical) profiles was comparable to typical CTD station spacing in most applications where data are used for geostrophic calculations and therefore a resultant velocity profile generated from a pair of Batfish profiles spaced at 10 km would be identical to and representative of a velocity profile obtained from a normal CTD survey. The difference, of course, was that the density of Batfish profile pairs (10 km apart) was very high with each pair and therefore each velocity profile was separated by ~0.5 km distance. It is emphasized here that each velocity profile represents a 10 km average and so by later plotting each successive profile separated by ~0.5 km distance, this will illustrate the sampling variability one can obtain from small displacements (~1 km) of the 10 km density pair. Resolution of the velocity structure will still only be on the scale of ~10 km.

Each geostrophic velocity profile was first calculated by integrating downward from the surface where the velocity (V surf.) was taken as zero. In deep oceans, the integration is usually carried out to the assumed depth of no motion; in this case, the maximum depth of the two was the limiting factor and the velocity at this level must be chosen to reference the velocity profile.

Current meters moored in our operational area were not recovered and therefore an absolute reference velocity could not be determined. A reference was chosen at 100 m depth with a velocity of $V_{ref} = -15$ (±5) cm s^{-1} (poleward) constant over the entire shelf. The depth of 100 m was chosen as it was the maximum depth sampled by the Batfish and horizontal variability was lower here than nearer the surface. The reference velocity itself [−15 cm s^{-1}] was chosen to be consistent with geostrophic calculations made here from CTD data taken from two cross shelf transects (9°S, 19°S) sampled approximately one week prior to and one week following the Batfish tows. The offshelf CTD stations extended to 500 m in depth but it was found that if this were used as the level of no motion, results inconsistent with historical and near area current meter data (Smith et al., 1978) were obtained and ancillary data were used to establish a velocity at 500 m (B. Towill, personal communication). The estimated reference velocity V_{ref} at 100 m was constant over the entire shelf width (~95 km) within the quoted error range of ±5 cm s^{-1}. The resultant shelf reference velocity was comparable in magnitude to geostrophic calculations (David Enfield, personal communication) which indicate a velocity of −10 cm s^{-1} (poleward) at ~100 m depth for a distance extending ~45 km from inshore (shelf width ~30 km). The latter calculations were made from data obtained at 15°S in July 1976. Wooster and Gilmartin (1961) also estimated geostrophic velocities of −4 cm s^{-1} and −20 cm s^{-1} (poleward) for stations ~100 km apart located at 8° and 10°30'S.

The geostrophic velocity profile, calculated using $V_{ref} = -15$ cm s^{-1}, for the across shelf transect is shown in Fig. 9. The velocity field was generated from ~100 velocity profiles calculated by the method previously described and subsequently contoured in steps of 5 cm s^{-1}. The cross-sectorial profile of velocity shown in Fig. 9 is designed to represent essentially a field of variability, which one would encounter when sampling a density pair separated by a typical CTD spacing of ~10 km. For example, if the 10 km density pair is centered at position 78°58'W (see Fig. 9), one obtains a near-surface velocity of ~−15 cm s^{-1}. For a density pair centered at 79°01'W or ~4 km from the last position (also representing ~20 min steaming time while towing Batfish), one

would estimate the near-surface flow at ~+5 cm s^{-1} (Fig. 9) which represents a considerable velocity difference. The absolute velocity field over the shelf is represented only on scales $\geqslant$ 10 km in Fig. 9 since each density pair represents an average profile over a 10 km distance. For example, the surface contour of 0 cm s^{-1} at position 78°55'W cannot be realistically resolved (at ~ 2 km) in Fig. 9; however, the two contours of 5 cm s^{-1} and 10 cm s^{-1} are reasonable estimates since they are measured on a much larger scale. The interpretation of the velocity cross-section between 78°50' to 78°55'W, simply stated, is that poleward flow decreases towards the surface and is near zero at the surface.

It is noted that the data gaps in the velocity contours of Fig. 9 do not correspond in position to the temperature and salinity data gaps of Figs. 2c and 3c, which are normally filled when calculating velocity profiles between pairs of Batfish tows as shown in the example of Fig. 8a. However, ~5 km of data are normally lost at either end of the calculations and therefore some data gaps necessarily remain. These gaps are shown by the three arrows on the left-hand side at 100 m depth indicating the dashed line contours. The velocity profiles within the section bounded by 78°55'W and 79°03'W in Fig. 7 were calculated from a Batfish transect made in the offshore direction 3 hr following the previous inshore transect ending at 78°50'W. It was more advantageous to use the long offshore transect since there were no data gaps remaining. The two arrows on the right-hand side at 100 m depth indicate the location where the velocity data were joined.

The velocity field in Fig. 9 was highly complex and indicated poleward flow with some near surface equatorward flow. For the most part the dashed line contours of the velocity field joined the data gaps in smooth fashion except for one section where the contours rose to the surface and large horizontal gradients were encountered. There are two possible explanations for this observation: either the change was a real spatial variation or a sampling problem, that is, a consequence of the time delay of ~2 hr between tows during which the velocity field changed. The latter case appeared to be more probable and this is discussed in the next section.

Fig. 9 The geostrophic velocity field generated for the across shelf Batfish transect at 9°20'S. Regions of data gaps have been joined by dashed line contours indicated from below by arrows. Equatorward flow is indicated by shaded area.

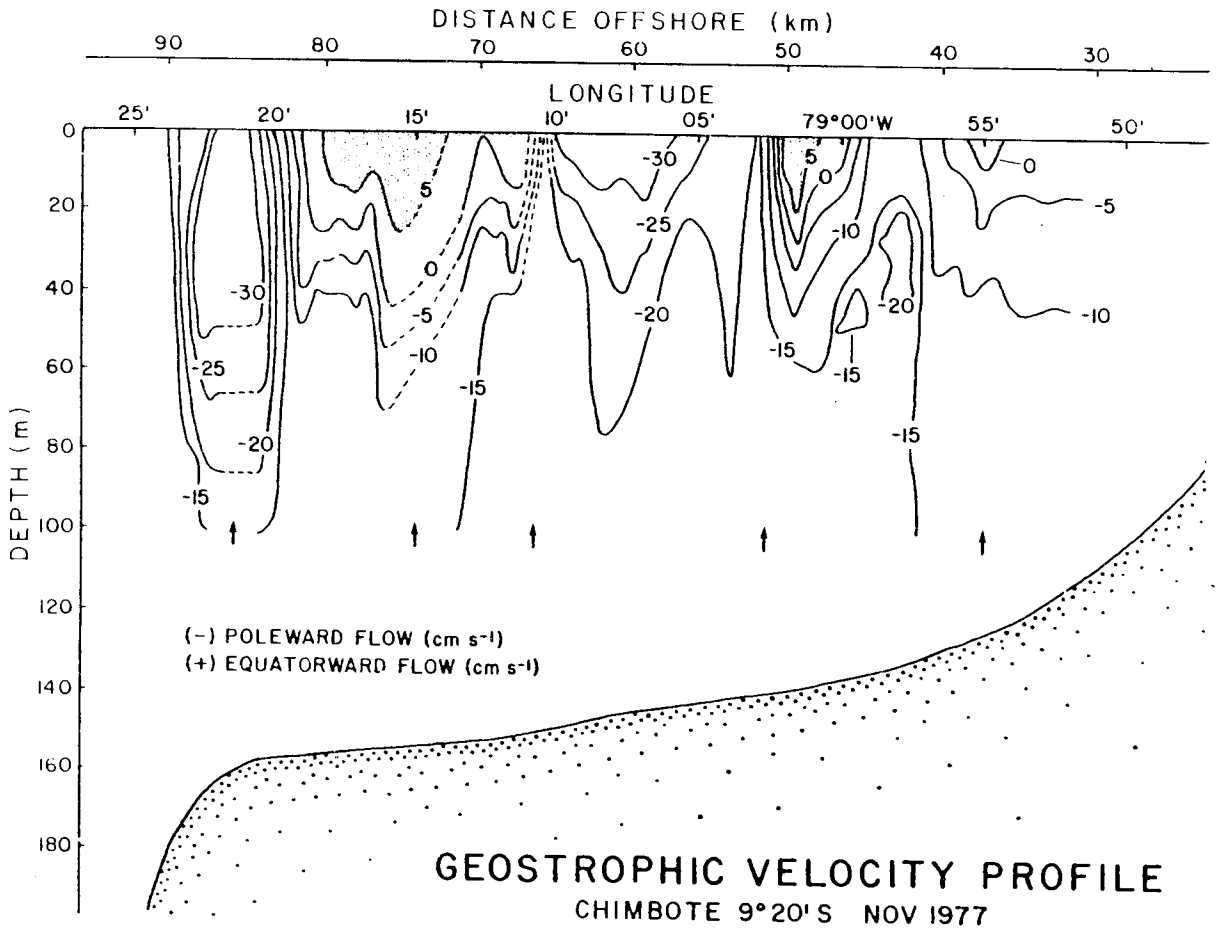

Temporal Variability of the Velocity Field. To investigate temporal variability, the region bounded by 78°55'W and 79°03'W (offshore tow) in Fig. 9 was subsequently reprofiled by the Batfish in two subsequent tows. The velocity field for all three transects encompassing a period of ~15 hr are shown in Fig. 10 (a,b,c). Fig. 10 (a) showed two lenses of surface water (shaded area) flowing equatorward and located at either end of the tow. Again it is noted here that the lens (shaded) at position 79°55'W of Fig. 9 was not resolved but only representative of decreasing poleward flow. Separating the two lenses from below was a region of strong poleward flow (~−20 cm s^{-1}). The velocity field shown in Fig. 9(b) had similar structure as the previous transect; however, it appeared slightly shifted onshore. Fig. 10(c) shows dramatic changes in the velocity field. The two lenses of equatorward flow were shifted offshore with considerable separation and the central region of the velocity field appeared to be stronger poleward flow. The question arises as to whether the fluctuations observed in Fig. 10 remained in geostrophic balance.

The time scales of these fluctuations were small (~5 hr) and therefore it is suggested that inertial effects may be important.

The simultaneous chlorophyll distributions measured for the three transects are shown in Fig. 10 (d,e,f). The length of each of the three tows were chosen to ensure that chlorophyll concentrations ⩾6 mg m^{-3} were measured at either end the tow and the low chlorophyll region in between obtained full spatial coverage. The chlorophyll field appeared correlated with changes in the velocity field in that the regions of high chlorophyll concentrations ⩾ 6 mg m^{-3} indicated by the shaded areas became separated during the last transect of Fig. 10(f). It would appear that the widening of the region of low chlorophyll in the last transect is a direct consequence of a water mass of different biological content being advected by an increase in poleward flow. The possibility also exists that the widening of the low chlorophyll region may have been a result of biological factors such as zooplankton grazing; however, these are less probable as the time scales required for such large decreases in chlorophyll are typically much longer than the time scales between transects (i.e. ~2 to 4 hr).

Fig. 10 (a,b,c) Three successive transects of ~20 n.m. in length along 9°20'S sampled over ~15 hr. The third transect indicated an increase in poleward flow.
(d,e,f) Corresponding profiles of chlorophyll.

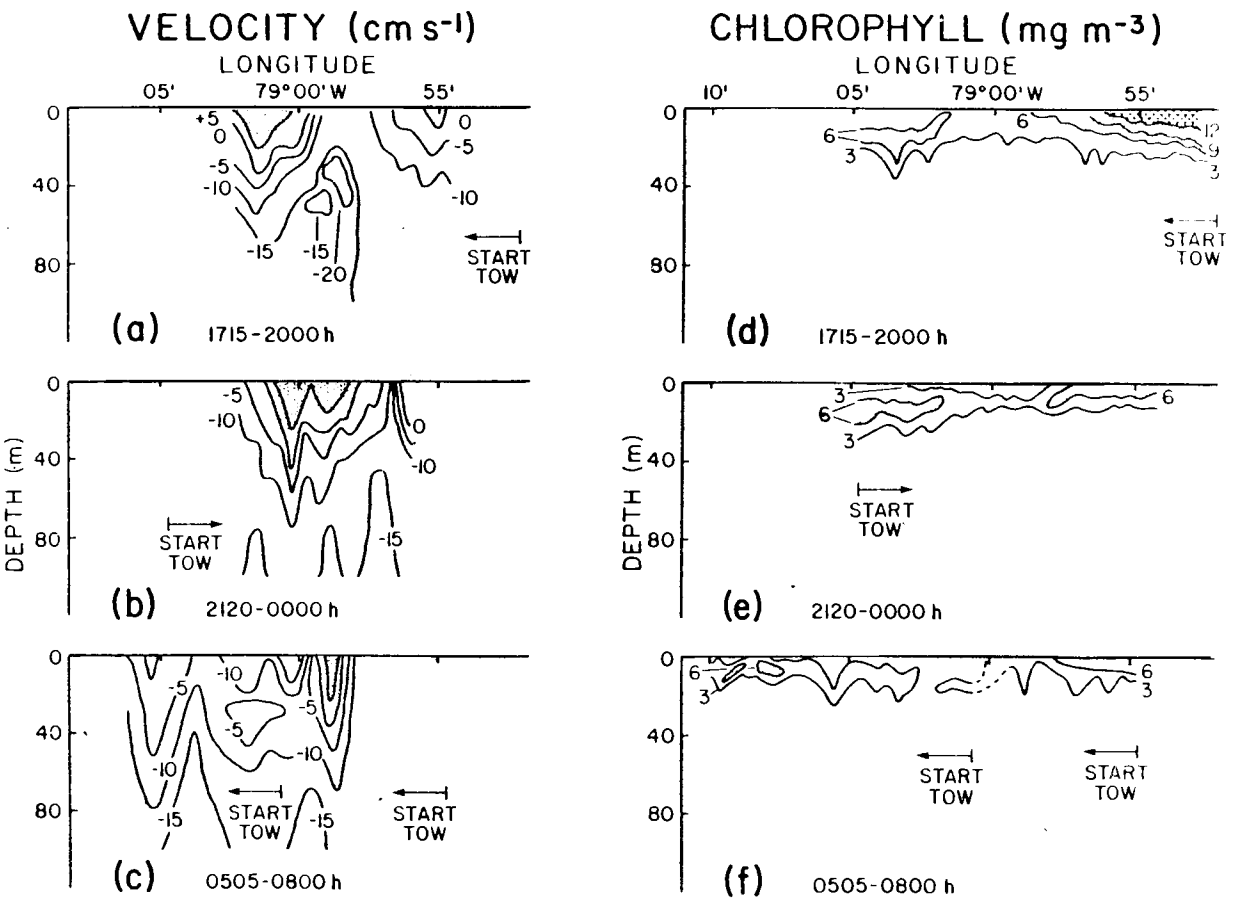

The estimated changes in the velocity field are indicative of the variability that could be measured temporally or spatially over the shelf (Fig. 9). Therefore the velocity profile in Fig. 9 must be regarded also as a time series where adjacent tows were representative of the velocity field only at time of sampling and point out the problem of estimating 'true' velocities in this area using vertical CTD profiles typically spaced at large distances of ~10 to 20 km where the existing fine structure and time scale changes could severly bias estimates of the true velocity field.

Vertical Stability. Potential vertical mixing mechanisms for nutrient transport were examined by estimating static and dynamic vertical stability over the Peru shelf in a similar manner to estimates made by Beers et al. (1971) at 15°S. These estimates may lend insight into the efficiency of vertical mixing of nutrients and the depth limits for productivity in the offshore and nearshore regions. Estimates of the Brunt-Väisälä frequency, N, were used as an indicator of static stability (assuming no vertical shear) where the possibility of weak vertical mixing was assumed to occur for small positive values of $N \leqslant 1 \times 10^{-3}$ s^{-1}. Estimates of N were generated from σ_t density profiles which were in turn generated from T,S profiles of Figs. 2 and 3. The distribution of Brunt-Väisälä frequencies over depth was determined from several density profiles for locations offshore (~79°16'W) and inshore (~78°50'W) and are plotted in Fig. 11 (a,b). Each point represents the Brunt-Väisälä frequency averaged over ~5 m depth intervals. The mean distribution of N versus depth was estimated by the curves shown in Fig. 11 (a,b). As expected from the temperature field in Fig. 2, vertical stability appeared highest in the upper layers ⩽50 m depth offshore and ⩽35 m inshore where the Brunt-Väisälä frequencies ranged from $N_B \sim 15 \times 10^{-3}$ s^{-1} in the stratified upper layers and $N_B \sim 2\text{–}3 \times 10^{-3}$ s^{-1} in the region below.

Dynamic stability was then examined for the same locations offshore and inshore by evaluating the Richardson number, Ri, the indicator of vertical shear instability. Mean vertical shears were estimated from the geostrophic velocity profiles corresponding to the contoured velocity field shown in Fig. 9 and were averaged over 10 m depth intervals. It is not clear that using vertical shears estimated from geostrophic calculations is a valid approach; however, they were used only as indicators and not in an absolute sense. The profiles of mean vertical shear are shown in Fig. 11 (c,d) for the offshore and inshore sections. The profiles indicated that the highest vertical shears were encountered inshore in the stratified upper layers and although values of shear were lower offshore, they decreased less rapidly with depth. The Richardson number Ri was subsequently obtained by evaluating the square of the Brunt-Väisälä frequency [Fig. 11 (a,b)] divided by the square of the vertical shear [Fig. 11 (c,d)], $N^2/(\partial v/\partial z)^2$, and the resulting profiles

Fig. 11 (a) The vertical profiles of the mean Vaisala frequency, N evaluated from several density profiles in the offshore and inshore regions. Each point was estimated over a 5 m interval and the curves represent the estimated mean profile.

(b) The vertical profiles of mean vertical shear averaged for two tows in the offshore and onshore regions. Each data point is averaged over 10 m intervals.

(c) The vertical profiles of mean Richardson number, Ri, estimated from the square of the Vaisala frequency divided by the square of the mena vertical shear. Ri decreases rapidly at ~50 and ~30 m for the offshore and onshore regions respectively separating the stratified upper layers from the upwelling waters.

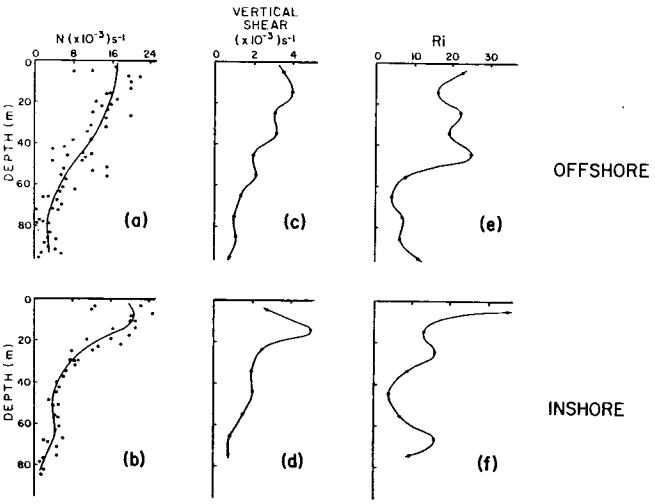

of Ri were plotted versus depth in Fig. 11 (e,f). The largest decrease and the lowest values (i.e. ⩽10) of Ri occurred at ⩽50 m depth in the offshore profile [Fig. 11 (e)] and ~30 m in the onshore profile [Fig. 11(f)]. This decrease was chosen as an approximate representation of the transtition region between high and low dynamic stability. The chlorophyll structure shown in Fig. 4 (c) was found just above the transition region of Ri in both the offshore and inshore sections where, for example, the contour of 3 mg m^{-3} was located at ~35 to 40 m depth offshore and ~25 m depth inshore. It appeared that the transition region of Ri separated the highly productive and stratified upper layers from upwelling waters. Within the upwelling waters, productivity was low even though nutrients were high (nitrate concentration >20 mg at m^{-3}). In the offshore region, one of the reasons that productivity exists at greater depths (~40 m) is due to the availability of nutrients brought in by efficient vertical mixing near the transition zone of Ri. However the depth region (~40 m) was light limited and any productivity would require the necessary condition that the phytoplankton populations be 'shade adapted' lending some support to

evidence for their existence on the shelf as proposed by Guillén and Rondan (1973).

SUMMARY

Physical processes operating on the Peru shelf at 9°S appear to dominate strongly the high variability in the physical and biological shelf structure. Both high speed sampling and synoptic coverage is required to obtain representative biological and physical profiles which adequately describe shelf activity. Geostrophic velocity calculations if at all valid for the Peru shelf, demonstrate high variability of the fine structure field on the order of Rossby radius scales of ~10 to 20 km and on short time scales of ~5 hrs. Estimates of shelf water transport based on geostrophic calculations should employ density profiles which include time averaging approximately over the inertial period of ~12 hrs.

Salinity was not only an indicator of water mass but appeared to be correlated with the chlorophyll maximum. The higher salinity water of ~35.1°/oo was identified as subtropical surface water which appeared to intrude over the shelf; however, it contained high chlorophyll concentrations yet moderate nutrient levels. This latter observation was inconsistent with previous shelf data.

Estimates of Richardson numbers may not have been calculated in a valid way by using geostrophic shears; however, they were used only as indicators for the predominance of vertical shear instabilities in vertical mixing. Poleward flow in this region is quite strong and would be consistent with large vertical shear instabilities. The estimates of Richardson numbers indicated that efficient vertical mixing occured deeper in the offshore regions and significant levels of chlorophyll were measured at greater depths. Production would have been light-limited unless phytoplankton populations were "shade-adapted" as proposed by Guillén and Rondan (1973).

ACKNOWLEDGEMENTS

The author wishes to thank Ken Drinkwater, Brian Petrie, Barry Towill, Glen Harrison and Ed Horne for their helpful discussions and critical comments of the manuscript. The efforts of the crew and officers of the CSS Baffin and the staff members of the Metrology Division during cruise #77030 are gratefully acknowledged: Messrs. P. Thorburn, S. Young and G. Dubois for their engineering, technical and computing assistance.

REFERENCES

BARBER, R.T., DUGDALE, J.J. MacISAAC, and R.L. SMITH. 1971. Variations in phytoplankton growth associated with the source and conditioning of upwelling water. **Inv. Pesq.** 35, 171-193.

BEERS, J.R., M.R. STEVENSON, R. W. EPPLEY, and E.R. BROOKS. 1971. Plankton populations and upwelling off the coast of Peru, June 1969. **Fish. Bull.** 69, Nº 4, 859-876.

BRINK, K.H., J.S. ALLEN, and R.L. SMITH. 1978. A study of low-freuquency fluctuaciones near the Peru Coast. **Journal of Physical Oceanography,** 8, 1025-1041.

DESSUREAULT, J.G. 1976. 'Batfish': A depth controllable towed body for collectiong oceanographic data. **Ocean Engineering,** 3, 99-111.

EBER, L.E., J.F.T. SAUR, and D.E. SETTE. 1968. Monthly mean charts: sea surface temperature North Pacific Ocean 1949-62. U.S. Bureau of Commercial Fisheries Circular 258.

GUILLEN, O., R. CALIENES, and R. de RONDAN. 1977. Medio ambiente y producción primaria frente al area, Pimentel-Chimbote. **Bol. Inst. Mar Perú Callao,** Vol. 3, Nº 4, 159 pp.

——— B.J. de MENDIOLA, and R.I. de RONDAN. 1973. Oceanography of the South Pacific 1972. Comp. R. Fraser. New Zealand National Commission for UNESCO, Wellington.

——— and R.I. RONDAN. 1973 Oceanography of the South Pacific 1972. comp. R. Fraser. New Zealand National Commission for UNESCO. Wellington.

HARRISON, W.G., T. PLATT, R. CALIENES, and N. OCHOA. 1980. Photosynthetic parameters and primary production of phytoplankton populations off the northern coast of Peru. To apper in the proceedings of the IDOE: International Symposium on Coastal Upwelling USC, 4-8 Feebruary 1980.

HERMAN, A.W. 1977. In situ chlorophyll and plankton measurements with a Batfish vehicle. MTS-IEEE Oceans '77 Conference Record, Session 39B: 1-5.

——— and T. M. DAUPHINEE . 1980. Continuous and rapid profiling of zooplankton with an electronic counter mounted on a 'Batfish' vehicle. **Deep-Sea Research,** 27, 79-96.

——— and K. L. DENMAN. 1976. Rapid underway profiling of chlorophyll with an in situ fluorometer mounted on a Batfish vehicle. **Deep-Sea Res.,** 24: 385-397.

NEUMAN, G., W.J. PEIRSON, JR. 1966. Principles of Physical Oceanography. Prentice-Hall, 54 pp.

POCKLINGTON, R., SMITH, and J. RICHMAN. 1977 Physical, chemical and biological data from fixed

stations: Part IV. Edited by L.A. Doe. A progress and data report on a Canada-Peru study of the Peruvian anchovy ecosystem. Bedford Institute of Oceanography Report Series, BI-R-078-6, Dartmouth, Nova Scotia, Canada, 211 pp.

RICHMAN,J.G., R. FLORES, E.P. HORNE, T. RIVERA, and B.W. TOWILL. 1978. Edited by L.A. Doe, A progress and data report on a Canada-Peru study of the Peruvian Anchovy and its ecosystem. Bedford Institute of Oceanography Report Series, BI-R-078-6, Dartmouth, N.S., Canada. 211 pp.

——— and S.L. SMITH. 1980. On the possible enchancement of oxygen depletion in the coastal waters of Peru between 6°S and 11°S. (In this volume.

SMITH,R.L., D.B. ENFIELD, T.S' HOPKINS, and R.D. PILLSBURY. 1971. The circulation in an upwelling ecosystem: The Pisco cruise. **Inv. Pesq.** 35, 9-24.

STRICKLAND, J.D.H., R.W. EPPLEY, and B.J. de MENDIOLA. 1969. Phytoplankton populations, nutrients and photosynthesis in Peruvian coastal waters. **Bol. Inst. Mar Peru Callao,** Vol. 2, N° 1, 45 pp.

WOOSTER, W.S., and M. GILMARTIN. 1971. The Peru-Chile undercurrent. **J. Mar. Res.,** 19: 97-122.

WYRTKI, K. 1963 The horizontal and vertical field of motion in the Peru current. Bulletin of the **Scripps Institution of Oceanography,** 8: 313-346.

YENTSCH, C.S., and D.W. MENZEL. 1963. A method for the determinaton of phytoplankton and phaeophytin by fluorescence. **Deep-Sea Res.,** 10:221-231.